HHS Public Access

Author manuscript

Cell Rep. Author manuscript; available in PMC 2018 April 25.

Published in final edited form as:

Cell Rep. 2018 April 03; 23(1): 255–269.e4. doi:10.1016/j.celrep.2018.03.077.

Molecular Characterization and Clinical Relevance of Metabolic Expression Subtypes in Human Cancers

Xinxin Peng[1,18], **Zhongyuan Chen**[1,2,18], **Farshad Farshidfar**[3,4,18], **Xiaoyan Xu**[5,1], **Philip L. Lorenzi**[1,6], **Yumeng Wang**[7,1], **Feixiong Cheng**[8,9], **Lin Tan**[1,6], **Kamalika Mojumdar**[1], **Di Du**[1], **Zhongqi Ge**[1], **Jun Li**[1], **George V. Thomas**[10], **Kivanc Birsoy**[11], **Lingxiang Liu**[12], **Huiwen Zhang**[13], **Zhongming Zhao**[14,15], **Calena Marchand**[16], **John N. Weinstein**[1,17], **The Cancer Genome Atlas Research Network**, **Oliver F. Bathe**[3,*], and **Han Liang**[1,17,7,19,*]

[1]Department of Bioinformatics and Computational Biology, The University of Texas MD Anderson Cancer Center, Houston, TX 77030, USA

[2]Department of Statistics, Rice University, Houston, TX 77005, USA

[3]Departments of Surgery and Oncology, University of Calgary, Calgary, T2N 4N2 Alberta, Canada

[*]Correspondence: bathe@ucalgary.ca (O.F.B.), hliang1@mdanderson.org (H.L.).
[18]These authors contributed equally
[19]Lead Contact

SUPPLEMENTAL INFORMATION

Supplemental Information includes six figures and three tables and can be found with this article online at https://doi.org/10.1016/j.celrep.2018.03.077.

AUTHOR CONTRIBUTIONS

O.F.B. and H.L. conceived and designed the study. X.P., Z.C., F.F., Y.W., F.C., D.D., Z.G., J.L., G.V.T., K.B., H.Z., Z.Z., C.M., J.N.W., O.F.B., and H.L. performed data analysis. X.X., P.L., L.T., and K.M. performed experiments. X.P., Z.C., F.F., F.C., O.F.B., and H.L. wrote the manuscript with inputs from other authors. H.L. supervised the whole project.

DECLARATION OF INTERESTS

Michael Seiler, Peter G. Smith, Ping Zhu, Silvia Buonamici, and Lihua Yu are employees of H3 Biomedicine, Inc. Parts of this work are the subject of a patent application: WO2017040526 titled “Splice variants associated with neomorphic sf3b1 mutants.” Shouyoung Peng, Anant A. Agrawal, James Palacino, and Teng Teng are employees of H3 Biomedicine, Inc. Andrew D. Cherniack, Ashton C. Berger, and Galen F. Gao receive research support from Bayer Pharmaceuticals. Gordon B. Mills serves on the External Scientific Review Board of Astrazeneca. Anil Sood is on the Scientific Advisory Board for Kiyatec and is a shareholder in BioPath. Jonathan S. Serody receives funding from Merck, Inc. Kyle R. Covington is an employee of Castle Biosciences, Inc. Preethi H. Gunaratne is founder, CSO, and shareholder of NextmiRNA Therapeutics. Christina Yau is a part-time employee/consultant at NantOmics. Franz X. Schaub is an employee and shareholder of SEngine Precision Medicine, Inc. Carla Grandori is an employee, founder, and shareholder of SEngine Precision Medicine, Inc. Robert N. Eisenman is a member of the Scientific Advisory Boards and shareholder of Shenogen Pharma and Kronos Bio. Daniel J. Weisenberger is a consultant for Zymo Research Corporation. Joshua M. Stuart is the founder of Five3 Genomics and shareholder of NantOmics. Marc T. Goodman receives research support from Merck, Inc. Andrew J. Gentles is a consultant for Cibermed. Charles M. Perou is an equity stock holder, consultant, and Board of Directors member of BioClassifier and GeneCentric Diagnostics and is also listed as an inventor on patent applications on the Breast PAM50 and Lung Cancer Subtyping assays. Matthew Meyerson receives research support from Bayer Pharmaceuticals; is an equity holder in, consultant for, and Scientific Advisory Board chair for OrigiMed; and is an inventor of a patent for EGFR mutation diagnosis in lung cancer, licensed to LabCorp. Eduard Porta-Pardo is an inventor of a patent for domainXplorer. Han Liang is a shareholder and scientific advisor of Precision Scientific and Eagle Nebula. Da Yang is an inventor on a pending patent application describing the use of antisense oligonucleotides against specific lncRNA sequence as diagnostic and therapeutic tools. Yonghong Xiao was an employee and shareholder of TESARO, Inc. Bin Feng is an employee and shareholder of TESARO, Inc. Carter Van Waes received research funding for the study of IAP inhibitor ASTX660 through a Cooperative Agreement between NIDCD, NIH, and Astex Pharmaceuticals. Raunaq Malhotra is an employee and shareholder of Seven Bridges, Inc. Peter W. Laird serves on the Scientific Advisory Board for AnchorDx. Joel Tepper is a consultant at EMD Serono. Kenneth Wang serves on the Advisory Board for Boston Scientific, Microtech, and Olympus. Andrea Califano is a founder, shareholder, and advisory board member of DarwinHealth, Inc. and a shareholder and advisory board member of Tempus, Inc. Toni K. Choueiri serves as needed on advisory boards for Bristol-Myers Squibb, Merck, and Roche. Lawrence Kwong receives research support from Array BioPharma. Sharon E. Plon is a member of the Scientific Advisory Board for Baylor Genetics Laboratory. Beth Y. Karlan serves on the Advisory Board of Invitae.

[4]Arnie Charbonneau Cancer Institute, University of Calgary, Calgary, T2N 4N1 Alberta, Canada

[5]Department of Pathophysiology, College of Basic Medicine Science, China Medical University, Shenyang, Liaoning Province 110122, China

[6]The Proteomics and Metabolomics Core Facility, The University of Texas MD Anderson Cancer Center, Houston, TX 77030, USA

[7]Graduate Program in in Quantitative and Computational Biosciences, Baylor College of Medicine, Houston, TX 77030, USA

[8]Center for Cancer Systems Biology and Department of Cancer Biology, Dana-Farber Cancer Institute, Boston, MA 02215, USA

[9]Center for Complex Networks Research and Department of Physics, Northeastern University, Boston, MA 02115, USA

[10]Department of Pathology and Laboratory Medicine, Oregon Health & Science University Knight Cancer Institute, Portland, OR 97239, USA

[11]Laboratory of Metabolic Regulation and Genetics, The Rockefeller University, New York, NY 10065, USA

[12]Department of Oncology, First Affiliated Hospital of Nanjing Medical University, Nanjing, Jiangsu 210029, China

[13]Department of Biochemistry and Molecular Biology, The University of Texas Health Science Center at Houston McGovern Medical School, Houston, TX 77030, USA

[14]Center for Precision Health, School of Biomedical Informatics, The University of Texas Health Science Center at Houston, Houston, TX 77030, USA

[15]Human Genetics Center, School of Public Health, The University of Texas Health Science Center at Houston, Houston, TX 77030, USA

[16]Faculty of Engineering, University of Waterloo, Waterloo, Ontario N2L 3G1, Canada

[17]Department of Systems Biology, The University of Texas MD Anderson Cancer Center, Houston, TX 77030, USA

SUMMARY

Metabolic reprogramming provides critical information for clinical oncology. Using molecular data of 9,125 patient samples from The Cancer Genome Atlas, we identified tumor subtypes in 33 cancer types based on mRNA expression patterns of seven major metabolic processes and assessed their clinical relevance. Our metabolic expression subtypes correlated extensively with clinical outcome: subtypes with upregulated carbohydrate, nucleotide, and vitamin/cofactor metabolism most consistently correlated with worse prognosis, whereas subtypes with upregulated lipid metabolism showed the opposite. Metabolic subtypes correlated with diverse somatic drivers but exhibited effects convergent on cancer hallmark pathways and were modulated by highly recurrent master regulators across cancer types. As a proof-of-concept example, we demonstrated that knockdown of *SNAI1* or *RUNX1*—master regulators of carbohydrate metabolic subtypes—modulates metabolic activity and drug sensitivity. Our study provides a system-level view of

metabolic heterogeneity within and across cancer types and identifies pathway cross-talk, suggesting related prognostic, therapeutic, and predictive utility.

In Brief

Peng et al. analyze a cohort of 9,125 TCGA samples across 33 cancer types to characterize tumor subtypes based on the expression of seven metabolic pathways. They find metabolic expression subtypes are associated with patient survivals and suggest the therapeutic and predictive relevance of subtype-related master regulators.

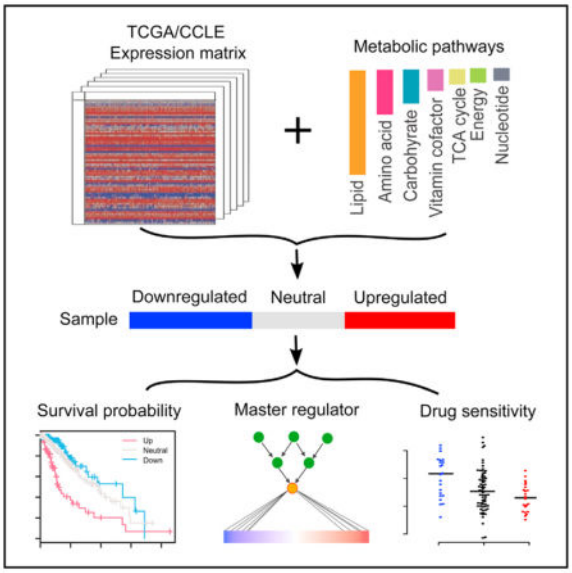

INTRODUCTION

Teleologically, cancer cells must modify their metabolic programs to adapt to the energy and macronutrient requirements that support rapid proliferation. Indeed, metabolic reprogramming is a well-established hallmark of cancer (Hanahan and Weinberg, 2011). For example, alterations in carbohydrate metabolism epitomized by the Warburg effect have been recognized for decades (Vander Heiden et al., 2009). Although different metabolic functions are known to be perturbed in cancer, studies of cancer metabolism usually focus on a specific perturbation and investigate it in isolation for a specific tumor type. However, metabolic reprogramming in tumor cells is complex, frequently consisting of alterations in several metabolic functions that synergize to promote tumorigenesis and cancer cell proliferation. Elucidating the full spectrum of metabolic reprogramming that occurs in human cancers will provide key insights into an essential aspect of tumor development and will also build a basis for the rational design of cancer treatments that target metabolism.

During carcinogenesis, somatic alterations in oncogenes and tumor suppressors transform cells by inducing broad gene expression changes that subsequently cause metabolic reprograming (Vander Heiden and DeBerardinis, 2017). Thus, gene expression represents a molecular dimension of particular interest in studying cancer metabolism since it bridges between oncogenic drivers and metabolic phenotypes. Some pioneering studies have

analyzed large-scale gene expression data across multiple cancer types (Haider et al., 2016; Hu et al., 2013; Nilsson et al., 2014; Reznik and Sander, 2015). Focusing on comparisons of tumor and adjacent normal tissue, those studies show widespread transcriptional dysregulation of metabolic genes. Although such studies have provided significant insight into altered metabolic pathways of cancer cells, the clinical relevance of the results may be limited since tumor and normal tissues usually contain very different cell compositions (e.g., fraction of epithelial cells). Gaude and Frezza (2016) took a more pertinent, pathway-focused approach to the analysis of data from clinical samples and identified several differentially expressed metabolic pathways that distinguish patients by clinical outcomes. Those and many other studies have revealed considerable metabolic heterogeneity, both within and among cancer types, underscoring the importance of patient stratification in a context-specific manner. However, it remains unclear how to stratify cancer patients most effectively into different subtypes (groups) based on the expression patterns of metabolic genes. More importantly, the utility of such tumor subtypes in guiding clinical practice and therapeutic development remains a major question. Here, using the comprehensive molecular data recently compiled in The Cancer Genome Atlas (TCGA) (Weinstein et al., 2013), we focused on seven metabolic super-pathways and characterized metabolic expression subtypes in 33 TCGA cancer types (9,125 samples; Table S1) to address those questions in a systematic way.

RESULTS

Expression Patterns of Metabolic Genes Reflect Metabolic Activities in Cancer Patients

To gain an incisive view of metabolic heterogeneity in cancer, we curated the gene sets of seven metabolic super-pathways based on the latest Reactome annotations (Fabregat et al., 2016). Included were amino acid metabolism (348 genes), carbohydrate metabolism (286 genes), integration of energy (110 genes), lipid metabolism (766 genes), nucleotide metabolism (90 genes), tricarboxylic acid cycle (TCA cycle, 148 genes) and vitamin & cofactor metabolism (168 genes) (Table S2). Those gene sets are largely independent of each other, with only a few genes of overlap, and they collectively represent major metabolic processes.

One key question is whether the expression patterns of metabolic pathway genes reflect actual metabolic activities in patients. Since data on the metabolites themselves are not available for TCGA samples, we obtained a published dataset that contains parallel metabolite profiling and gene expression data on 60 breast cancer patient samples (Terunuma et al., 2014) and focused on the 296 metabolites that had been annotated to 6 out of the 7 metabolic super-pathways that we surveyed. For each metabolite, we calculated the correlation of its abundance with gene expression levels in the corresponding metabolic pathway, then compared the resultant p value distribution with the background distribution calculated from other genes (Figure 1A). In total, we detected 73 metabolites that significantly correlated with the expression of corresponding metabolic pathway genes (false discovery rate [FDR] < 0.15), including 22 metabolites involved in amino acid metabolism, 22 in carbohydrate metabolism, 21 in nucleotide metabolism, 4 in vitamin & cofactor metabolism, 2 in integration of energy, and 2 in lipid metabolism (Figure 1B shows four

representative cases from different pathways; Figure 1C provides the full list of significant metabolites). To assess the statistical significance of the number of significant hits detected, we performed a simulation analysis to compare the number of metabolites with significant signals from each pathway with those based on random gene sets of the same size. Strikingly, all six metabolic pathways showed higher numbers of significant metabolites than expected by chance ($p < 0.05$, Figure 1D). For example, the number of significant carbohydrate metabolites for the real pathway gene set was 22, whereas the expected number for a random gene set was only 0.3 ($p < 0.001$). These results indicate that the expression patterns of metabolic pathway genes do reflect metabolic activities.

Classification of Metabolic Expression Subtypes and Their Overall Similarity

We next aimed to characterize metabolic heterogeneity within cancer types based on the expression patterns of metabolic pathway genes. For that purpose, we developed a computational method to classify tumor samples into "directional" metabolic subtypes in two independent steps (Figure 2A). In the first step, within each cancer type, we normalized gene expression across samples by Z score to obtain a rank value for each gene (~18,000 coding genes) within each sample. Then, given the gene set of a specific metabolic pathway, we conducted gene set enrichment analysis (GSEA) (Subramanian et al., 2005) on the resulting rank values to classify tumors into three subtypes: (1) "upregulated subtype" for the samples in which metabolic pathway genes showed enrichment with high Z scores (FDR < 0.25); (2) "downregulated subtype" for samples showing the opposite pattern (FDR < 0.25); and (3) "neutral subtype" for samples showing no significant enrichment pattern. Note that the concept of "upregulated" or "downregulated" here is relative to other tumors within the same cancer type, rather than relative to normal tissues. In the second step, we assessed whether the metabolic genes overall showed differential expression patterns (FDR < 0.05) among the tumor subtypes defined in the first step, given that metabolic expression subtypes were expected to capture the variation in metabolic pathway gene expression. Among 231 cases assessed (7 pathways × 33 cancer types), 93.9% of the cases (217) met that criterion and were kept for subsequent analyses.

Using the method described above for each metabolic pathway, we classified 9,125 samples into the three subtypes. Figure 2B shows the relative proportions of those subtypes across and within cancer types. Figure S1 shows metabolic genes with the most consistent changes among the subtypes across cancer types. Based on the subtype information, we further examined the co-occurrence of expression subtypes of different metabolic pathways and found that many subtype combinations occurred at a much higher frequency than expected by chance (Figure 2C). For example, the most common subtype combination was those with upregulated amino acid metabolism, nucleotide metabolism, and TCA cycle. They showed >10-fold more frequently than expected by chance (Figure 2D). We compared the similarity of different metabolic subtype classifications based on sample-level labels and found that amino acid metabolism, TCA cycle, and nucleotide metabolism formed one tight cluster, whereas integration of energy, carbohydrate metabolism, lipid metabolism, and vitamin & cofactor metabolism formed another distinct cluster (Figure 2E). These results provide a global view of the similarity of different metabolic pathways and may reflect crosstalk among them.

Metabolic Expression Subtypes Show Extensive Clinically Relevant Patterns

To assess the clinical relevance of the metabolic expression subtypes identified above, we next determined correlations with patient overall survival, since survival represents a key clinical index of tumor aggressiveness. Figure 3A is a summary of 33 significant survival associations for the metabolic subtypes in 27 cancer types that included sufficient sample size and follow-up time (log-rank test, FDR < 0.2, 28 associations remained significant after adjusting for tumor purity). Notably, upregulated subtypes of carbohydrate, nucleotide, and vitamin & cofactor metabolism were consistently associated with poor prognosis (Figure 3B), compatible with the hypothesis that cancer cells have increased demands for glucose uptake and nucleotide synthesis (Pavlova and Thompson, 2016; Vander Heiden and DeBerardinis, 2017). Unexpectedly, upregulated TCA cycle and lipid metabolic subtypes were associated with better prognosis (Figure 3C). Amino acid metabolism and energy integration subtypes showed mixed patterns. We obtained similar results using univariate Cox regression models (Figure S2). The consistent association of survival patterns with certain metabolic subtypes (e.g., carbohydrate metabolism) across cancer types suggests that metabolic subtyping has potential prognostic value.

Among the cancer types surveyed, low-grade glioma (LGG) exhibited the most extensive survival correlations (5 out of the 7 metabolic pathways; Figure S3). For LGG, poor prognosis was significantly associated with downregulated subtypes of amino acid metabolism, energy integration, and TCA cycle but with upregulated subtypes of carbohydrate and vitamin & cofactor metabolism. LGGs have mutations of isocitrate dehydrogenase 1 (*IDH1*) in >70% of cases and mutations of *IDH2* in a minority of cases. *IDH1* and *IDH2* mutations are activating for production of high levels of the oncometabolite 2-hydroxygluta-rate (2HG) from alpha-ketoglutarate (Claus et al., 2015; Dang et al., 2009; Ward et al., 2010). The extensive prognostic patterns observed support the notion of glioma as a disease influenced by metabolism.

Genomic profiling studies, especially recent TCGA studies, have characterized a number of tumor subtypes that capture major patterns of within-disease heterogeneity. Those tumor subtypes are informative about cancer pathophysiology and, in some cases, for clinical decision making. We therefore examined the correlations between metabolic expression subtypes and previously established molecular tumor subtypes and detected many significant correlations (Figure S4). For example, in breast invasive carcinoma (BRCA), we found that the vast majority of cases in which nucleotide metabolism was downregulated belonged to the luminal A (lumA) subtype (Sørlie et al., 2001); in esophageal carcinoma (ESCA), cases with upregulated lipid and vitamin & cofactor metabolism were enriched in the chromosomal instability subtype (CIN) (Cancer Genome Atlas Research Network, 2017); in glioblastoma multiforme (GBM), cases of downregulated lipid metabolism were enriched in the IDHmut-non-codel subtype (Eckel-Passow et al., 2015); in head-neck squamous cell carcinoma (HNSC), cases with downregulated carbohydrate metabolism were enriched in the HPV^{-} subtype (Figure 3C). These results highlight the clinical relevance of metabolic expression subtypes presented here and provide an informative metric for defining tumor heterogeneity.

Metabolic Expression Subtypes Are Associated with Diverse Somatic Drivers but Convergent Pathway Functional Effects

Metabolic reprogramming can be largely viewed as a consequence of oncogenic driver events (DeBerardinis and Chandel, 2016). For example, mutated *TP53* and *MYC* amplification have been extensively linked to anabolic or catabolic activities, including glycolysis and redox balance in cancer (Kruiswijk et al., 2015; Stine et al., 2015). To identify somatic alterations that potentially drive metabolic expression subtypes, we performed a correlation analysis of metabolic expression subtypes with mutation driver genes. For each cancer type, we identified significantly mutated genes (SMGs, identified by MutSigCV, with a mutation frequency >5%) (Lawrence et al., 2013) and assessed whether their mutation status correlated with metabolic subtypes. We found 31 associated SMGs (chi-square test, FDR < 0.05), and their associated patterns were quite diverse across cancer types (Figure 4A). The SMGs identified recurrent across multiple cancer types included *TP53* (9 cancer types), *PIK3CA* (4 cancer types), *KRAS* (3 cancer types), *CDH1* (2 cancer types), *CTNNB1* (2 cancer types), *EGFR* (2 cancer types), *HRAS* (2 cancer types), *IDH1* (2 cancer types), *KEAP1* (2 cancer types), and *NFE2L2* (2 cancer types). Figure 4B shows the metabolic subtype correlations with mutated *TP53* as an example. Similarly, we examined the correlations of metabolic expression subtypes with potential drivers of somatic copy number alteration (SCNA). For each cancer type, we identified amplified oncogenes or deleted tumor suppressors in SCNA peaks (identified by GI-SITC2, FDR < 0.25) (Mermel et al., 2011) and assessed whether their copy number status correlated with a metabolic subtype (chi-square test, FDR < 0.05). We identified 35 such drivers. Some of them showed correlations with multiple metabolic subtypes in several cancer types, including *ARID1A* (8 cancer types), *MYC* (7 cancer types), *CDKN2A* (6 cancer types), *EGFR* (5 cancer types), *PARK2* (5 cancer types), *RB1* (4 cancer types), *PTEN* (4 cancer types), *AKT1* (4 cancer types), *BCL2L1* (4 cancer types), and *SOX2* (4 cancer types; Figure 4C). Figure 4D shows the subtype correlations with amplified *MYC* as an example. These analyses provide a broad view of potential somatic drivers associated with metabolic reprogramming in human cancer.

To assess further the biological relevance of metabolic expression subtypes, we examined their associations with various cellular pathways by GSEA based on mRNA expression (FDR < 0.01, Figure 4E). That analysis included six functional cancer hallmarks (i.e., angiogenesis, apoptosis, DNA repair, epithelial–mesenchymal transition [EMT], G2M checkpoint, and inflammatory response) and also the mTORC1 signaling pathway, which has been implicated in metabolic dysregulation and cancer development (Hay, 2016) (STAR Methods). Interestingly, despite the diversity of cancer types surveyed, we found that pathway-level functional effects associated with each kind of metabolic subtype were largely consistent across cancer types. Among the seven metabolic expression subtypes, amino acid metabolism, nucleotide metabolism, and TCA cycle exhibited the most similar profiles. Their upregulated subtypes were consistently associated with increased DNA repair, decreased angiogenesis, decreased EMT, and decreased inflammation (Figure 4E). Angiogenesis, EMT, and inflammation were positively correlated with upregulated carbohydrate metabolism and integration of energy and, to a lesser degree, upregulated lipid metabolism and metabolism of vitamins & cofactors. G2M checkpoint was consistently

negatively correlated with the energy and lipid metabolism subtypes. DNA repair was inversely correlated with energy integration and lipid metabolism. Interestingly, mTORC1 signaling was generally increased for all of the metabolic subtypes except energy integration, consistent with the central role of mTORC1 signaling in regulating cancer metabolism. Overall, these results suggest that metabolic activity is intrinsically coupled with cancer hallmark pathways.

Highly Recurrent Master Regulators for Metabolic Subtypes across Cancer Types

To elucidate how the metabolic expression subtypes are regulated, we performed computational analyses to identify two types of “master regulators”: transcription factors (TFs) and miRNAs (STAR Methods). For TFs (Figure 5A), we first inferred tumor-context-specific gene regulatory networks based on the cancer-type-specific expression data, using the algorithm for reconstruction of accurate cellular networks (ARACNe) (Lachmann et al., 2016). We then employed the master regulator inference algorithm (MARINa) and the shadow analysis (Aytes et al., 2014; Lefebvre et al., 2010) to infer the master TFs for each metabolic pathway in each cancer type. The analysis revealed many highly recurrent TFs for the same metabolic pathway across different cancer types. Among different metabolic subtypes, amino acid metabolism, nucleotide metabolism, and TCA cycle shared a large number of master TFs across many cancer types (Figure 5B).

For miRNAs, we used two criteria to identify master regulators: (1) the miRNA targets are significantly enriched in differentially expressed genes between upregulated and downregulated subtypes and (2) the miRNAs themselves show significant corresponding changes between the two subtypes (STAR Methods). We found that many miRNA master regulators recurred across cancer types. miR-484, miR-107, miR-320a, and miR-429 appeared to be the strongest regulators of the metabolism of amino acids, nucleotides, carbohydrates, and vitamins & cofactors. Interestingly, the latter three miRNAs have been reported to be key regulators of cancer metabolism (Chan et al., 2015; Rottiers and Näär, 2012) (Figure 5C). Further examination revealed that SCNAs can modulate the expression of some regulators, such as miR-320a in stomach adenocarcinoma (STAD) for nucleotide metabolic expression subtypes (Figure 5D).

A Systematic View of Altered Metabolism in Cancer

Integrating insights from the above analyses, a systematic view of heterogeneous metabolic activity in cancer has emerged (Figure 6A). Metabolic reprogramming may result from diverse somatic driver alterations in different tumor contexts, but it appears to converge on common pathway-level functional effects through modulation of highly recurrent master regulators across cancer types, ultimately leading to consistent survival patterns. According to this model, the master TFs identified here are key nodes with the greatest influence on systems-level metabolic activities. Therefore, those TFs may represent a class of therapeutic targets whose inhibition could potentially yield clinical benefits.

To test that hypothesis, we focused on carbohydrate metabolism, since its upregulated subtypes showed the most consistently poor prognostic patterns across cancer types (Figures 3A and 3B). To be an ideal target, a master TF should be more highly expressed in the

subtype with worse prognosis so that inhibition and subsequent downregulation of the target could confer enhanced survival. Among the 8 cancer types whose upregulated carbohydrate subtypes had significantly worse survival rates, four master TFs, *SNAI1*, *RUNX1*, *RUNX2*, and *FOSL1*, were identified in at least three cancer types (Figure 6B). We chose two TFs, *SNAI1* and *RUNX1*, to perform experimental perturbation. Figures 6C and 6D show higher expression levels of those two genes in the upregulated subtypes in lung adenocarcinoma (LUAD) and sarcoma (SARC), respectively. Using shRNAs, we knocked down the expression of *SNAI1* in a lung cancer cell line, NCIH1975, and *RUNX1* in a sarcoma cell line, U2OS (Figure S5, Table S3). We then measured the relative abundance of intracellular glucose (a model carbohydrate) using high-resolution mass spectrometry at time points of 0 h, 6 h, and 24 h. The concentrations of intracellular glucose were significantly decreased in the knockdown cell lines (Figure 6E and F, paired t test, $p < 0.05$), suggesting that *SNAI1* and *RUNX1* indeed positively modulate carbohydrate metabolism. Further studies with more robust controls will be required to validate the proposed effects in terms of whether the knockdown affects glucose transporter expression and whether the knockdown has predicted effects on carbohydrate metabolic gene expression.

Metabolic Expression Subtypes Are Informative About Drug Sensitivity

To explore further the potential clinical utility of carbohydrate metabolic expression subtypes, we used expression and drug sensitivity data from Cancer Cell Line Encyclopedia (CCLE) (Barretina et al., 2012; Iorio et al., 2016). We focused on 181 lung cancer cell lines because of the sufficient sample size for subtype classification. Using the same bioinformatic methods as described above, we classified 34, 33, and 114 cell lines as down-regulated, upregulated, and neutral subtypes, respectively. We next compared the molecular characteristics associated with up-regulated subtypes of patient samples and cell lines. *EGFR*—the most important therapeutic target in lung cancer—was identified as a SCNA driver associated with carbohydrate metabolic expression subtypes of patient samples. It showed significantly higher copy-number and mRNA expression levels in the upregulated carbohydrate subtype than in the downregulated subtype (Figure S6A). Concordantly, the carbohydrate expression subtypes of lung cancer cell lines adhered to that pattern (Figure S6B). Furthermore, the cell lines in the upregulated subtype had higher proliferation rates than those from the downregulated subtype (Figure S6C), consistent with the observation that LUAD patients in the upregulated carbohydrate metabolic subtype exhibited worse prognosis (Figure 3B) (Haverty et al., 2016). These results independently validate the patterns observed in TCGA patient samples, suggesting that the analyses are robust.

Given the three carbohydrate expression subtypes of lung cancer cell lines, we found that 12 drugs showed significantly different sensitivities (Figure 7A, FDR < 0.05). Among those drugs, docetaxel is a chemotherapy drug currently used for patients with lung cancer. Cell lines in the carbohydrate-upregulated subtype were more sensitive to docetaxel than cell lines in other subtypes (Figure 7B). To test further the effect of carbohydrate metabolism on drug sensitivity, we assessed the sensitivity of lung cancer cell line NCIH1975 (classified as upregulated subtype) to knockdown of *SNAI1*, since that perturbation has been found to modulate carbohydrate metabolism negatively. Indeed, compared with the negative control (scrambled shRNA), the *SNAI1*-KD cell line was more resistant to docetaxel, and that

pattern was consistently observed at both 16 hr and 24 hr after treatment (Figures 7C and 7D). The results suggest that LUAD patients with high carbohydrate metabolic activities may be more likely to benefit from docetaxel treatment.

DISCUSSION

Metabolic reprogramming is considered one of the hallmarks of cancer (Hanahan and Weinberg, 2011; Ward and Thompson, 2012). Because metabolism is so complex, there is a need for systematic characterization. Several previous studies have demonstrated considerable heterogeneity in the expression of genes involved in various metabolic functional pathways (Gaude and Frezza, 2016; Haider et al., 2016; Hu et al., 2013; Nilsson et al., 2014; Reznik and Sander, 2015). Based on a breast cancer patient cohort with parallel metabolite and transcriptomic profiling data (Terunuma et al., 2014), we demonstrated that the expression patterns of metabolic pathways indeed reflect metabolic activities. Metabolite profiling has recently become an informative approach to elucidate tumor heterogeneity (Hakimi et al., 2016). Similar analyses should extend to more patient cohorts to further validate our findings when such data are available.

The expression patterns analyzed in previous studies ranged from global to discrete (i.e., affecting particular metabolic pathways). Here, we have focused on effective stratification of cancers based on the expression heterogeneity of metabolic genes within cancer types. One central aim is to define meaningful metabolic expression subtypes. Our computational method, which combines GSEA and self-contained gene set analysis, has two advantages: (1) it allows consistent classification of tumor subtypes, facilitating comparison and contrast across a broad range of cancer types and (2) it classifies tumor samples according to “functional state” of a specific metabolic process (upregulated, neutral, or downregulated), facilitating interpretation of downstream analyses. Through that systematic classification, we found that metabolic expression subtypes frequently correlate with each other. In particular, metabolic perturbations of amino acids, nucleotides, and TCA cycle are strongly coupled, as demonstrated by high correlations of their subtype assignment, similar pathway-level associations, and shared master regulators. That global perspective has not been presented previously. Another feature of the present study is that, by integrating TCGA multidimensional molecular data on the same sample cohorts, we have identified potential drivers and master regulators associated with the metabolic derangements observed in our global analysis. While the driver roles of some alterations identified in affecting metabolism such as *TP53* mutation and *MYC* amplification have been documented, further efforts will be required to validate the causal relationships of others.

The metabolic expression subtypes defined here have potential clinical implications. First, we demonstrate the extensive correlations of metabolic expression subtypes with prognosis across cancer types, suggesting that the subtypes reflect essential aspects of tumor development. Notably, different metabolic expression subtypes showed distinct patterns. The upregulated subtypes of carbohydrates, nucleotides, and vitamins & cofactors were associated with worse prognosis, whereas lipid metabolism showed the opposite association. Regardless of underlying reasons, that observation suggests a more complex relationship between metabolic reprogramming and cell proliferation than usually assumed. Second,

using CCLE data, we demonstrate that the metabolic subtypes correlate with sensitivity to drugs used in the clinic, highlighting the possibility that metabolic status will sometimes be important to consider in selection of a treatment regime. Overall, the results here support the potential utility of metabolic expression subtypes as prognostic and predictive markers.

Since metabolic reprogramming is an essential aspect of tumorigenesis and cancer cell proliferation, inhibition of metabolic functions may inhibit tumor progression. Current strategies for considering the effect of metabolism on therapy focus on functionally important metabolic isoenzymes that show cancer-specific somatic or expression changes. There have been a number of studies along those lines (Vander Heiden and DeBerardinis, 2017), but targeting of metabolic genes for therapy has had only very limited success (Vander Heiden and DeBerardinis, 2017). Our systems-biological analysis suggests a generic therapeutic strategy. For upregulated metabolic subtypes that are consistently associated with worse patient prognosis, tumors may be vulnerable to a therapy, or component of combination therapy, that targets their master regulatory factors. Inhibiting responsible master regulators has the potential to convert the upregulated subtype to the downregulated subtype, thereby conferring a survival benefit. Our functional validation results provide preliminary but exciting evidence supporting that hypothesis, and further studies will be required.

STAR★METHODS

Key Resource Table

REAGENT or RESOURCE	SOURCE	IDENTIFIER
Chemical, Peptides, and Recombinant Proteins		
RPMI 1640	Corning, NY, USA	Cat#10-040-CV
Fetal bovine serum	GIBCO	Cat#16140-071
DMEM with 4.5 g/L glucose, L-glutamine, & sodium pyruvate	Corning, NY, USA	Cat#10-013-CV
Puromycin	GIBCO	Cat#A1113803; CAS:58-58-2
Docetaxel	ENZO, New York, USA	Cat#BML-T129; CAS: 114977-28-5
DMSO	MP Biomedicals LLC, France	Cat#02196055; CAS: 67-68-5
Formic acid	VWR	EM-FX0440-5
Acetonitrile	Fisher Scientific	A955-4
Methanol	Fisher Scientific	A456-4
Acetic acid	Fisher Scientific	A38-212
Chemical Commercial Assays		
High-Capacity cDNA Reverse Transcription Kit	Applied Biosystems, CA, USA	Cat#4374967
RNeasy Plus Mini Kit	QIAGEN, Hilden, Germany	Cat#74136
SYBR(R) Select Master Mix Life technologies, CA, USA	Applied Biosystems, CA, USA	Cat#4472908
Deposited Data		

REAGENT or RESOURCE	SOURCE	IDENTIFIER
TCGA gene expression data	Genomic Data Commons	https://gdc.cancer.gov/about-data/publications/pancanatlas
TCGA somatic mutation data	Genomic Data Commons	https://gdc.cancer.gov/about-data/publications/pancanatlas
TCGA somatic copy number alteration data	Genomic Data Commons	https://gdc.cancer.gov/about-data/publications/pancanatlas
TCGA miRNA-seq data	Genomic Data Commons	https://gdc.cancer.gov/about-data/publications/pancanatlas
TCGA patient clinic data and purity data	Genomic Data Commons	https://gdc.cancer.gov/about-data/publications/pancanatlas
Experimental Models: Cell lines		
Human: NCIH1975 cells	Laboratory of Dr. Zahid H. Siddik, MD Anderson Cancer Center, TX, USA	N/A
Human: U2OS cells	MD Anderson Characterized Cell Line Core Facility, TX, USA	N/A
Human: HEK293LTX	MD Anderson Characterized Cell Line Core Facility, TX, USA	N/A
Oligonucleotides		
shRNA targeting *RUNX1* and *SNAI1*	Table S3, this paper	N/A
Primers for quantitative PCR	Table S4, this paper	N/A
Recombinant DNA		
MISSION® TRC2 pLKO.5-puro Non-Mammalian shRNA Control Plasmid DNA	Sigma-Aldrich, MO, USA	Cat#SHC202
PLKO-puro shRNA constructs	Sigma-Aldrich, MO, USA	Refer to Table S3
Lentiviral Packaging Mix psPAX2 and pMD2.G	Addgene, MA, USA	Plasmid# 12260 and 12259
Software and Algorithms		
Gene Set Enrichment Analysis (GSEA)	(Mootha et al., 2003; Subramanian et al., 2005)	http://software.broadinstitute.org/gsea/index.jsp
ARACNe	(Lachmann et al., 2016)	https://sourceforge.net/projects/aracne-ap/
ssmarina	(Aytes et al., 2014; Lefebvre et al., 2010)	https://figshare.com/articles/ssmarina_R_system_package/785718
Thermo TraceFinder	ThermoFisher Scientific	https://www.thermofisher.com/order/catalog/product/OPTON-30491

CONTACT FOR REAGENT AND RESOURCE SHARING

Further information and requests for resources and reagents should be directed to and will be fulfilled by the Lead Contact, Han Liang (hliang1@mdanderson.org).

EXPERIMENTAL MODEL AND SUBJECT DETAILS

The NCIH1975 cell line was a generous gift from Dr. Zahid H. Siddik's laboratory at MD Anderson Cancer Center. HEK293LTX and U2OS cell lines were obtained from MD Anderson Characterized Cell Line Core Facility. All cell lines were confirmed by short tandem repeat (STR) analysis and were negative for mycoplasma contamination prior to use. NCIH1975 cells were cultured in RPMI 1640 medium supplemented with 10% fetal bovine

serum. U2OS cells were maintained in DMEM with L-glutamine, 4.5 g/L glucose, sodium pyruvate and 10% fetal bovine serum.

METHOD DETAILS

Analysis of metabolic pathway genes and metabolite profiling data in breast cancer samples—We obtained metabolite profiling data and mRNA expression data on 60 breast cancer patients (Terunuma et al., 2014). We focused the 296 metabolites that had been annotated to the 6 metabolic super pathways including 88 in amino acid, 38 in carbohydrate, 9 in integration of energy, 116 in lipid metabolism, 26 in nucleotide, and 19 in vitamin & cofactor metabolism. For each metabolite, we calculated the Spearman rank correlations between its abundance and the expression levels of the genes in the corresponding pathway. Then we compared the empirical cumulative distributions of p values from pathway genes versus other genes using Kolmogorov-Smirnov test. One-tailed test was used to test whether the p values of the pathway gene set were more significant than those of other genes at FDR < 0.15. To evaluate whether pathway genes are more informative about metabolic activities than other gene sets, we performed a simulation analysis. We randomly selected a gene set with the same size of a metabolic pathway and identified the number of metabolites significantly correlated with the expression of the gene set in the same way as the metabolic pathway genes. We repeated this analysis for 1,000 times to generate the background distribution of significant hits from which we assessed the observed numbers were statistically higher than random expectation.

Metabolic expression subtype classification—Considering the heterogeneity of the metabolic pathway dysregulation in tumors, we developed an algorithm to classify individual tumors given the gene set of each metabolic pathway. For a specific patient, the classification was based on the deviation extent of the expression level of genes in a metabolic functional pathway from the average values of the cohort relative to other genes. For each of the 33 cancer types, Z-normalization was performed per gene across samples. Then, the genes were ranked by Z scores per sample. GSEA pre-ranked analysis was used to determine whether the genes from a metabolic pathway were enriched at the top or bottom of the pre-ranked gene list for each sample. For a specific pathway, a tumor sample was classified into one of three distinct groups at FDR < 0.25: “upregulated,” “downregulated,” or “neutral.” Then we performed self-contained gene analysis to confirm each subtype classification. Given the metabolic expression subtypes, we first evaluated expression differentiation of protein-coding genes using ANOVA and then used the Kolmogorov-Smirnov test to determine whether the p values of the pathway genes were lower than those from other genes (FDR < 0.05). Through this systematic analysis, each tumor sample was labeled with seven kinds of metabolic expression subtypes. To determine the mutual dependence among those seven classifications, mutual information was calculated using the R package “entropy.” After normalizing the mutual information by dividing the maximum value for each row, the mutual information distance was calculated as 1- mutual information.

Clinical relevance analysis of metabolic expression subtypes—We evaluated the correlations of metabolic expression subtypes with two clinical features respectively: the patients’ overall survival time and established molecular subtype. The R package “survival”

was used to perform the overall survival analysis and produce Kaplan-Meier survival plots. A log-rank test was used to assess the significance (FDR < 0.2). For significant survival associations, we further assessed whether the subtypes correlated with tumor purity using ANOVA or whether the survival correlations remained significant after including tumor purity as covariate in Cox model. As for molecular subtype analysis, chi-square test was performed to access the correlation between tumor subtypes and metabolic expression subtypes (assigned to one of three values, −1, 0, or 1, FDR < 0.05).

Somatic driver association analysis—To identify oncogenic events that potentially drive metabolic reprogramming, we analyzed the associations of mutation drivers and SCNA drivers with metabolic expression subtypes in each cancer type. For the mutation analysis, we first excluded 314 hypermutated samples, and only focused on the significantly mutated genes (identified by MutSigCV 1.4, FDR < 0.25) (Lawrence et al., 2013) with a mutation frequency > 5% for each cancer type. We performed chi-square test to determine the association between the metabolic expression subtypes and a specific mutated gene status, and reported the significance at FDR < 0.05. For the SCNA analysis, we assessed the copy number status of known oncogenes or tumor suppressors (Zack et al., 2013) residing in a significant amplification or deletion peak identified by GISTIC2 (Mermel et al., 2011) in each cancer type by chi-square test (FDR < 0.05).

Biological pathway association analysis—To explore the biological processes responsible for the metabolic reprogramming, we analyzed the correlations between metabolic expression subtypes with cancer hallmark pathways in each cancer type. The $\log_2$ transformed RNA-seq data were used. The seven selected cancer hallmark pathways were angiogenesis, apoptosis, DNA repair, EMT, G2M checkpoint, inflammatory response and mTORC1 signaling, and the related gene sets were obtained from MSigDB (http://software.broadinstitute.org/gsea/msigdb). We used Student's t tests between upregulated and downregulated subtypes to generate ranked gene lists for each cancer type. Then, pre-ranked GSEA analysis were used to determine the pathway enrichment or depletion (FDR < 0.01).

Master regulator analysis—To identify TF master regulators, we first inferred the tumor-context-specific GRNs with the expression data (*Z* score transformed) from all tumor samples using ARACNe-AP, which is a new Java implementation of the ARACNe (Lachmann et al., 2016). Our analysis used the list of transcription factors as previously described (Vaquerizas et al., 2009). Then, given the inferred networks, we used the MARINa (R package *ssmarina*) to infer master regulators based on the comparison of expression between upregulated and down-regulated samples for each metabolic expression subtype in each cancer type and performed the shadow analysis to all master regulators identified with p < 0.05 (Aytes et al., 2014; Lefebvre et al., 2010). We identified master TFs as those passing the shadow analysis (FDR < 0.1) and having ≥150 target genes. To identify miRNA master regulators, we used two criteria: (1) the expression level of the microRNA itself showed a significant difference between the two groups (fold-change > 1.2 and p value < 0.01); and (2) the miRNA target genes that showed differential expression between upregulation and downregulation subtypes were prone to being commonly regulated by a specific microRNA (FDR < 0.1). GSEA (including annotated miRNA target gene sets) was

employed for this analysis (Subramanian et al., 2005); and the differential direction of the microRNA should be opposite to the expression of the corresponding target gene set. The network of master regulators and metabolic subtypes were analyzed by Cytoscape (Shannon et al., 2003). In the TF networks, each link represented a specific TF identified in at least 3 cancer types. As for miRNA, a link represented a specific microRNA identified in at least one cancer type.

Analysis of CCLE data—We downloaded RNaseq-based expression data and gene-level copy number from Cancer Cell Line Encyclopedia (CCLE; https://portals.broadinstitute.org/ccle) and focused on 181 lung cancer cell lines with gene expression data. Using the same classification pipeline, we classified them into downregulated, neutral, and upregulated subtypes based on the expression levels from the carbohydrate pathway. We obtained the drug screening data from Iorio et al. (2016). We performed ANNOVA analysis to determine whether (log-transformed) IC_{50} values showed significant difference among the three carbohydrate expression subtypes of cell lines (FDR < 0.05). We obtained the doubling time data of cancer cell lines from Haverty et al. (2016). We used Wilcoxon rank sum test to assess whether the doubling time showed a significant difference between carbohydrate downregulated and upregulated subtypes.

Generation of stable cell lines—Lentiviruses were produced by co-transfection HEK293LTX cells with the MISSION® TRC2 pLKO.5-puro Non-Mammalian shRNA Control Plasmid DNA or with the pLKO-puro shRNA constructs (Sigma, shRNA sequences are available in Table S3) and the Lentiviral Packaging Mix (psPAX2 and pMD2.G). U2OS and NCIH1975 cells were transduced by the lentivirus, and cells with stable knockdowns were selected using puromycin (2 μg/ml for U2OS and 1 μg/ml for NCIH1975). The knockdown of *RUNX1* and *SNAI1* in stable cell lines was confirmed by quantitative real-time PCR.

RNA isolation and quantitative real-time PCR—To examine the effect of the knockdown on potential target genes, total RNA was isolated using the RNeasy Plus Mini Kit (QIAGEN, Hilden, Germany) and transcribed into cDNA using the High-Capacity cDNA Reverse Transcription Kit (Applied Biosystems, CA, USA). Reactions were performed in triplicates using the SYBR®Select Master Mix (Applied Biosystems) and specific primers (Sigma, sequences are available in Table S3). RT-qPCR was performed on an Applied Biosystems 7900HT Fast Real-Time PCR system (Applied Biosystems). The gene expression levels were normalized to β-actin, and relative expression was calculated by the $2^{(-DDCt)}$ method.

Glucose measurement by IC-HRMS—We measured the intracellular abundance of glucose in cell samples using high-resolution mass spectrometry (HRMS) as follows. Cells were seeded in 10 cm dishes and incubated in fresh medium (DMEM or RPMI-1640 containing 10% or 5% FBS, respectively) for 0 hr, 6 hr, and 24 hr. Before conducting cell extraction, media samples were collected, flash frozen using liquid nitrogen, and transferred to −80°C freezer until analysis. Cells were then quickly washed with ice-cold PBS flowed by Milli-Q water to remove extra salt/medium components. Metabolites were then extracted

by adding 500 μL 1% formic acid in 90/10 (v/v) acetonitrile/water. Cell and medium extracts were then centrifuged at 17,000 *g* for 5 min at 4°C, and supernatants were transferred to clean tubes. Samples were evaporated to dryness using a SpeedVac. Samples were reconstituted in deionized water, then 10 μL was injected into a Thermo Scientific Dionex ICS-5000+ capillary ion chromatography (IC) system containing a Thermo IonPac AS11 250 × 2 mm with 4 μm particle size. IC flow rate was 300 μl/min (at 30°C) and the gradient conditions were as follows: initial 1 mM KOH, increased to 35 mM at 25 min, then to 99 mM at 39 min, held 99 mM for 10 min. The total run time was 50 min. Methanol containing 2 mM acetic acid was delivered by an external pump and mixed with the eluent. Data were acquired using a Thermo Orbitrap Fusion Tribrid Mass Spectrometer under ESI negative mode. Thermo Trace Finder software was used for metabolite identification and area integration. The abundance of glucose was normalized by dividing the area of each metabolite by the total signal (summed areas of all metabolites) for each sample.

Drug sensitivity assays—To assess changes in drug sensitivity following *SNAI1* knockdown, stable cells (1,500 per well) were seeded in 96-well plates in the complete medium a day before treatment. A 2 mM stock solution of docetaxel (ENZO, New York, USA) was prepared in DMSO and was further diluted in complete medium to obtain eight serial dilutions such that the final treatment concentrations ranged from 0–2 μM. *SNAIL*-KD cells and the negative control (scrambled shRNA) cells were treated with DMSO or the various docetaxel dilutions and cell viability was determined using live imaging (Incucyte Zoom, Essen Biosciences). Phase contrast images (4x objective) were recorded at 0 hr, 16 hr and 24 hr after treatment initiation and the percentage confluence (a measure of cell viability) was assessed using the associated software as per manufacturer's instructions. Relative viability was normalized to the confluence value treated with DSMO. Docetaxel treatment was repeated independently to ensure reproducibility of the results. The Student's t test was used to analyze differences, and $p < 0.05$ was considered statistically significant.

QUANTIFICATION AND STATISTICAL ANALYSIS

All the analyses were based on 9,125 tumor samples except for miRNA (7,939) due to limited data availability. Definition of significance of various statistical tests were described and referenced in their respective Method Details sections.

DATA AND SOFTWARE AVAILABILITY

The raw data, processed data and clinical data can be found at the legacy archive of the GDC (https://portal.gdc.cancer.gov/legacy-archive/search/f) and the PancanAtlas publication page (https://gdc.cancer.gov/about-data/publications/pancanatlas). The mutation data can be found here (https://gdc.cancer.gov/about-data/publications/mc3-2017). TCGA data can also be explored through the Broad Institute FireBrowse portal (http://gdac.broadinstitute.org) and the Memorial Sloan Kettering Cancer Center cBioPortal (http://www.cbioportal.org). Details for software availability are in the Key Resource Tables.

Supplementary Material

Refer to Web version on PubMed Central for supplementary material.

Acknowledgments

This study was supported by grants from the U.S. National Institutes of Health (R01CA175486 and U24CA209851 to H.L., U54HG003273, U54HG003067, U54HG003079, U24CA143799, U24CA143835, U24CA143840, U24CA143843, U24CA143845, U24CA143848, U24CA143858, U24CA143866, U24CA143867, U24CA143882, U24CA143883, U24CA144025, P30CA016672); grants from the Cancer Prevention and Research Institute of Texas (RP140462 to H.L. and RP130397 that supports the Metabolomics Core Facility); and a University of Texas System STARS award (to H.L.). We thank the MD Anderson high-performance computing core facility for computing, Dr. Zahid H. Siddik for providing NCIH1975 cell line, and LeeAnn Chastain for editorial assistance.

References

Aytes A, Mitrofanova A, Lefebvre C, Alvarez MJ, Castillo-Martin M, Zheng T, Eastham JA, Gopalan A, Pienta KJ, Shen MM, et al. Cross-species regulatory network analysis identifies a synergistic interaction between FOXM1 and CENPF that drives prostate cancer malignancy. Cancer Cell. 2014; 25:638–651. [PubMed: 24823640]

Barretina J, Caponigro G, Stransky N, Venkatesan K, Margolin AA, Kim S, Wilson CJ, Lehár J, Kryukov GV, Sonkin D, et al. The Cancer Cell Line Encyclopedia enables predictive modelling of anticancer drug sensitivity. Nature. 2012; 483:603–607. [PubMed: 22460905]

Cancer Genome Atlas Research Network; Analysis Working Group: Asan University; BC Cancer Agency; Brigham and Women's Hospital; Broad Institute; Brown University; Case Western Reserve University; Dana-Farber Cancer Institute; Duke University; et al. Integrated genomic characterization of oesophageal carcinoma. Nature. 2017; 541:169–175. [PubMed: 28052061]

Chan B, Manley J, Lee J, Singh SR. The emerging roles of microRNAs in cancer metabolism. Cancer Lett. 2015; 356(2 Pt A):301–308. [PubMed: 25451319]

Claus EB, Walsh KM, Wiencke JK, Molinaro AM, Wiemels JL, Schildkraut JM, Bondy ML, Berger M, Jenkins R, Wrensch M. Survival and low-grade glioma: the emergence of genetic information. Neurosurg Focus. 2015; 38:E6.

Dang L, White DW, Gross S, Bennett BD, Bittinger MA, Driggers EM, Fantin VR, Jang HG, Jin S, Keenan MC, et al. Cancer-associated IDH1 mutations produce 2-hydroxyglutarate. Nature. 2009; 462:739–744. [PubMed: 19935646]

DeBerardinis RJ, Chandel NS. Fundamentals of cancer metabolism. Sci Adv. 2016; 2:e1600200. [PubMed: 27386546]

Eckel-Passow JE, Lachance DH, Molinaro AM, Walsh KM, Decker PA, Sicotte H, Pekmezci M, Rice T, Kosel ML, Smirnov IV, et al. Glioma Groups Based on 1p/19q, IDH, and TERT Promoter Mutations in Tumors. N Engl J Med. 2015; 372:2499–2508. [PubMed: 26061753]

Fabregat A, Sidiropoulos K, Garapati P, Gillespie M, Hausmann K, Haw R, Jassal B, Jupe S, Korninger F, McKay S, et al. The Reactome pathway Knowledgebase. Nucleic Acids Res. 2016; 44(D1):D481–D487. [PubMed: 26656494]

Gaude E, Frezza C. Tissue-specific and convergent metabolic transformation of cancer correlates with metastatic potential and patient survival. Nat Commun. 2016; 7:13041. [PubMed: 27721378]

Haider S, McIntyre A, van Stiphout RG, Winchester LM, Wigfield S, Harris AL, Buffa FM. Genomic alterations underlie a pan-cancer metabolic shift associated with tumour hypoxia. Genome Biol. 2016; 17:140. [PubMed: 27358048]

Hakimi AA, Reznik E, Lee CH, Creighton CJ, Brannon AR, Luna A, Aksoy BA, Liu EM, Shen R, Lee W, et al. An integrated metabolic atlas of clear cell renal cell carcinoma. Cancer Cell. 2016; 29:104–116. [PubMed: 26766592]

Hanahan D, Weinberg RA. Hallmarks of cancer: the next generation. Cell. 2011; 144:646–674. [PubMed: 21376230]

Haverty PM, Lin E, Tan J, Yu Y, Lam B, Lianoglou S, Neve RM, Martin S, Settleman J, Yauch RL, Bourgon R. Reproducible pharmacogenomic profiling of cancer cell line panels. Nature. 2016; 533:333–337. [PubMed: 27193678]

Hay N. Reprogramming glucose metabolism in cancer: can it be exploited for cancer therapy? Nat Rev Cancer. 2016; 16:635–649. [PubMed: 27634447]

Hu J, Locasale JW, Bielas JH, O'Sullivan J, Sheahan K, Cantley LC, Vander Heiden MG, Vitkup D. Heterogeneity of tumor-induced gene expression changes in the human metabolic network. Nat Biotechnol. 2013; 31:522–529. [PubMed: 23604282]

Iorio F, Knijnenburg TA, Vis DJ, Bignell GR, Menden MP, Schubert M, Aben N, Gonçalves E, Barthorpe S, Lightfoot H, et al. A Landscape of Pharmacogenomic Interactions in Cancer. Cell. 2016; 166:740–754. [PubMed: 27397505]

Kruiswijk F, Labuschagne CF, Vousden KH. p53 in survival, death and metabolic health: a lifeguard with a licence to kill. Nat Rev Mol Cell Biol. 2015; 16:393–405. [PubMed: 26122615]

Lachmann A, Giorgi FM, Lopez G, Califano A. ARACNe-AP: gene network reverse engineering through adaptive partitioning inference of mutual information. Bioinformatics. 2016; 32:2233–2235. [PubMed: 27153652]

Lawrence MS, Stojanov P, Polak P, Kryukov GV, Cibulskis K, Sivachenko A, Carter SL, Stewart C, Mermel CH, Roberts SA, et al. Mutational heterogeneity in cancer and the search for new cancer-associated genes. Nature. 2013; 499:214–218. [PubMed: 23770567]

Lefebvre C, Rajbhandari P, Alvarez MJ, Bandaru P, Lim WK, Sato M, Wang K, Sumazin P, Kustagi M, Bisikirska BC, et al. A human B-cell interactome identifies MYB and FOXM1 as master regulators of proliferation in germinal centers. Mol Syst Biol. 2010; 6:377. [PubMed: 20531406]

Mermel CH, Schumacher SE, Hill B, Meyerson ML, Beroukhim R, Getz G. GISTIC2.0 facilitates sensitive and confident localization of the targets of focal somatic copy-number alteration in human cancers. Genome Biol. 2011; 12:R41. [PubMed: 21527027]

Mootha VK, Lindgren CM, Eriksson KF, Subramanian A, Sihag S, Lehar J, Puigserver P, Carlsson E, Ridderstråle M, Laurila E, et al. PGC-1α-responsive genes involved in oxidative phosphorylation are coordinately downregulated in human diabetes. Nat Genet. 2003; 34:267–273. [PubMed: 12808457]

Nilsson R, Jain M, Madhusudhan N, Sheppard NG, Strittmatter L, Kampf C, Huang J, Asplund A, Mootha VK. Metabolic enzyme expression highlights a key role for MTHFD2 and the mitochondrial folate pathway in cancer. Nat Commun. 2014; 5:3128. [PubMed: 24451681]

Pavlova NN, Thompson CB. The Emerging Hallmarks of Cancer Metabolism. Cell Metab. 2016; 23:27–47. [PubMed: 26771115]

Reznik E, Sander C. Extensive decoupling of metabolic genes in cancer. PLoS Comput Biol. 2015; 11:e1004176. [PubMed: 25961905]

Rottiers V, Näär AM. MicroRNAs in metabolism and metabolic disorders. Nat Rev Mol Cell Biol. 2012; 13:239–250. [PubMed: 22436747]

Shannon P, Markiel A, Ozier O, Baliga NS, Wang JT, Ramage D, Amin N, Schwikowski B, Ideker T. Cytoscape: a software environment for integrated models of biomolecular interaction networks. Genome Res. 2003; 13:2498–2504. [PubMed: 14597658]

Sørlie T, Perou CM, Tibshirani R, Aas T, Geisler S, Johnsen H, Hastie T, Eisen MB, van de Rijn M, Jeffrey SS, et al. Gene expression patterns of breast carcinomas distinguish tumor subclasses with clinical implications. Proc Natl Acad Sci USA. 2001; 98:10869–10874. [PubMed: 11553815]

Stine ZE, Walton ZE, Altman BJ, Hsieh AL, Dang CV. MYC, Metabolism, and Cancer. Cancer Discov. 2015; 5:1024–1039. [PubMed: 26382145]

Subramanian A, Tamayo P, Mootha VK, Mukherjee S, Ebert BL, Gillette MA, Paulovich A, Pomeroy SL, Golub TR, Lander ES, Mesirov JP. Gene set enrichment analysis: a knowledge-based approach for interpreting genome-wide expression profiles. Proc Natl Acad Sci USA. 2005; 102:15545–15550. [PubMed: 16199517]

Terunuma A, Putluri N, Mishra P, Mathé EA, Dorsey TH, Yi M, Wallace TA, Issaq HJ, Zhou M, Killian JK, et al. MYC-driven accumulation of 2-hydroxyglutarate is associated with breast cancer prognosis. J Clin Invest. 2014; 124:398–412. [PubMed: 24316975]

Vander Heiden MG, DeBerardinis RJ. Understanding the Intersections between Metabolism and Cancer Biology. Cell. 2017; 168:657–669. [PubMed: 28187287]

Vander Heiden MG, Cantley LC, Thompson CB. Understanding the Warburg effect: the metabolic requirements of cell proliferation. Science. 2009; 324:1029–1033. [PubMed: 19460998]

Vaquerizas JM, Kummerfeld SK, Teichmann SA, Luscombe NM. A census of human transcription factors: function, expression and evolution. Nat Rev Genet. 2009; 10:252–263. [PubMed: 19274049]

Ward PS, Patel J, Wise DR, Abdel-Wahab O, Bennett BD, Coller HA, Cross JR, Fantin VR, Hedvat CV, Perl AE, et al. The common feature of leukemia-associated IDH1 and IDH2 mutations is a neomorphic enzyme activity converting alpha-ketoglutarate to 2-hydroxyglutarate. Cancer Cell. 2010; 17:225–234. [PubMed: 20171147]

Ward PS, Thompson CB. Metabolic reprogramming: a cancer hallmark even warburg did not anticipate. Cancer Cell. 2012; 21:297–308. [PubMed: 22439925]

Weinstein JN, Collisson EA, Mills GB, Shaw KR, Ozenberger BA, Ellrott K, Shmulevich I, Sander C, Stuart J. Cancer Genome Atlas Research Network. The Cancer Genome Atlas Pan-Cancer analysis project. Nat Genet. 2013; 45:1113–1120. [PubMed: 24071849]

Zack TI, Schumacher SE, Carter SL, Cherniack AD, Saksena G, Tabak B, Lawrence MS, Zhsng CZ, Wala J, Mermel CH, et al. Pan-cancer patterns of somatic copy number alteration. Nat Genet. 2013; 45:1134–1140. [PubMed: 24071852]

Highlights

- Classification of metabolic expression subtypes in 33 TCGA cancer types
- Metabolic expression subtypes show consistent prognostic patterns across cancer types
- Analysis of master regulators of metabolic subtypes suggesting therapeutic targets
- Metabolic expression subtypes associated with sensitivity to drugs in clinical use

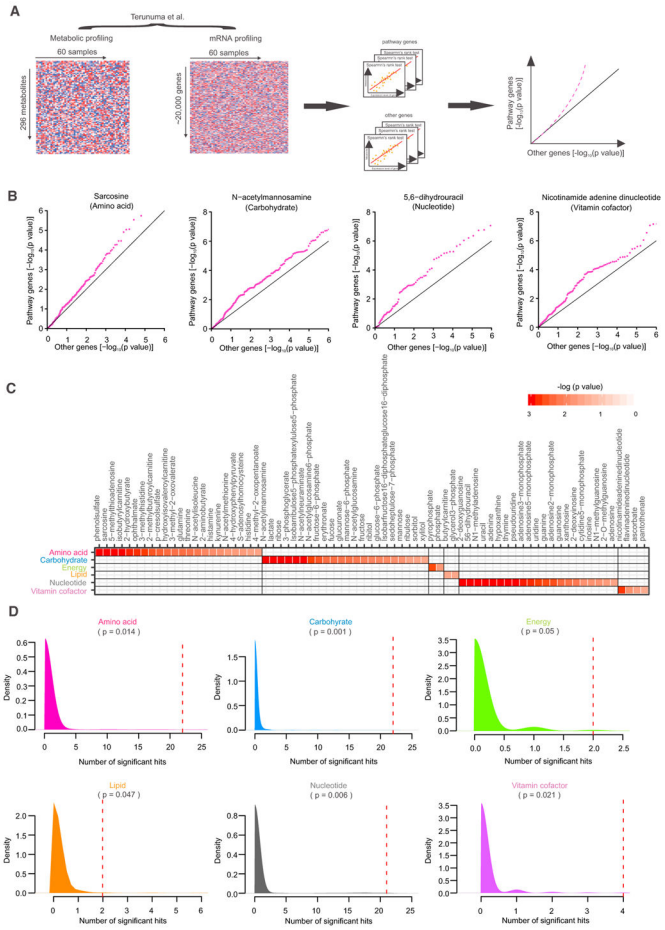

Figure 1. The Expression Patterns of Metabolic Pathway Genes Reflect Metabolite Levels in Cancer Patient Samples

(A) The analytic pipeline for assessing whether the expression levels of metabolic pathway genes are correlated with the concentration of a given metabolite.

(B) Representative quantile-quantile (QQ) plots showing p values (log transformed) from the metabolite-gene Spearman correlation coefficients of pathway genes compared to other genes. Sarcosine for amino acid metabolism; N-acetylmannosamine for carbohydrate metabolism; 5, 6-dihydrouracil for nucleotide metabolism; nicotinamide adenine dinucleotide for vitamin & cofactor metabolism.

(C) Heatmap showing all metabolites whose intracellular concentrations significantly correlate with the expression levels of the corresponding pathway genes (FDR < 0.15).

(D) The statistical significance of the numbers of metabolites correlated with the pathway gene expression based on the background distribution of random gene sets. The red lines indicate the true numbers.

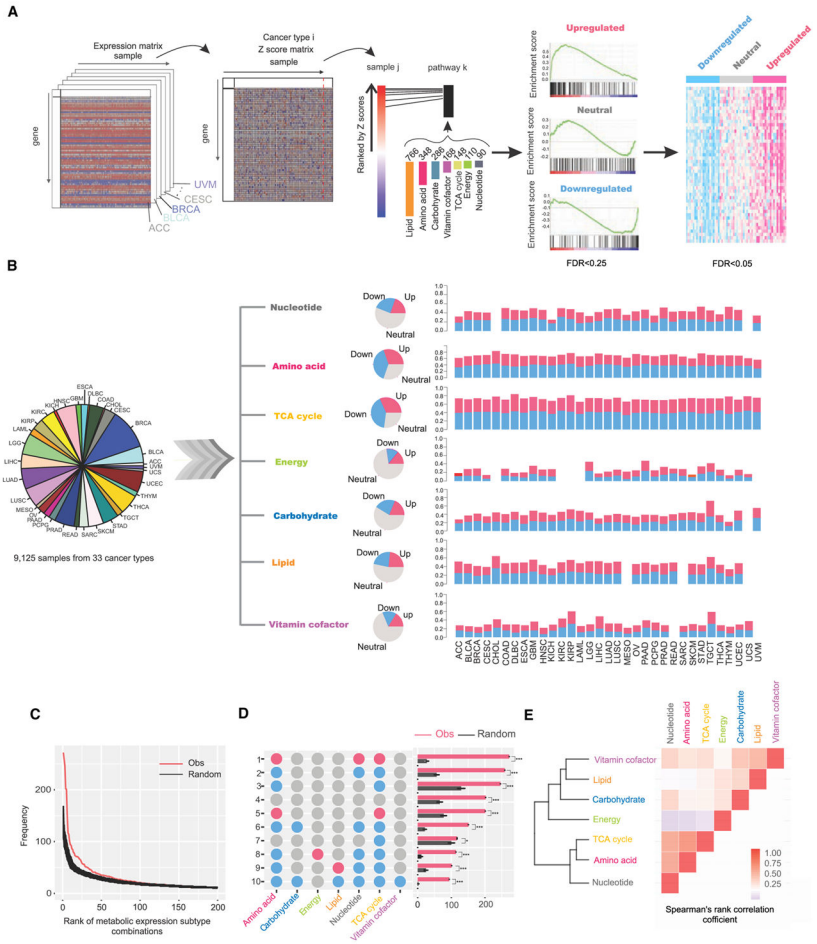

Figure 2. Classification of Metabolic Expression Subtypes Based on Pathway Gene Expression

(A) The computational method to classify tumor samples into three metabolic expression subtypes: upregulated, downregulated, and neutral. Bar charts represent the numbers of genes for metabolic pathways surveyed.

(B) Distributions of three metabolic subtypes for each metabolic pathway in 33 cancer types. Only tumor subtype classifications passing the two-step statistical criteria in (A) are shown.

(C) Frequency distribution of a specific metabolic subtype combination. The red line is for the observed distribution; black lines are for the random expectation assuming that each metabolic pathway is perturbed independently in a tumor sample.

(D) The top 10 most frequently observed metabolic subtype combinations. Red, upregulated subtype; gray, neutral subtype; and blue, downregulated subtype. The right panel indicates the observed and expected frequencies of a specific subtype combination. Data are represented as mean ± SD. *$p < 0.05$, ***$p < 0.001$.

(E) Clustering pattern of the seven metabolic subtypes based on the similarity of subtype labels across 9,125 samples.

See also Table S1, Table S2, and Figure S1.

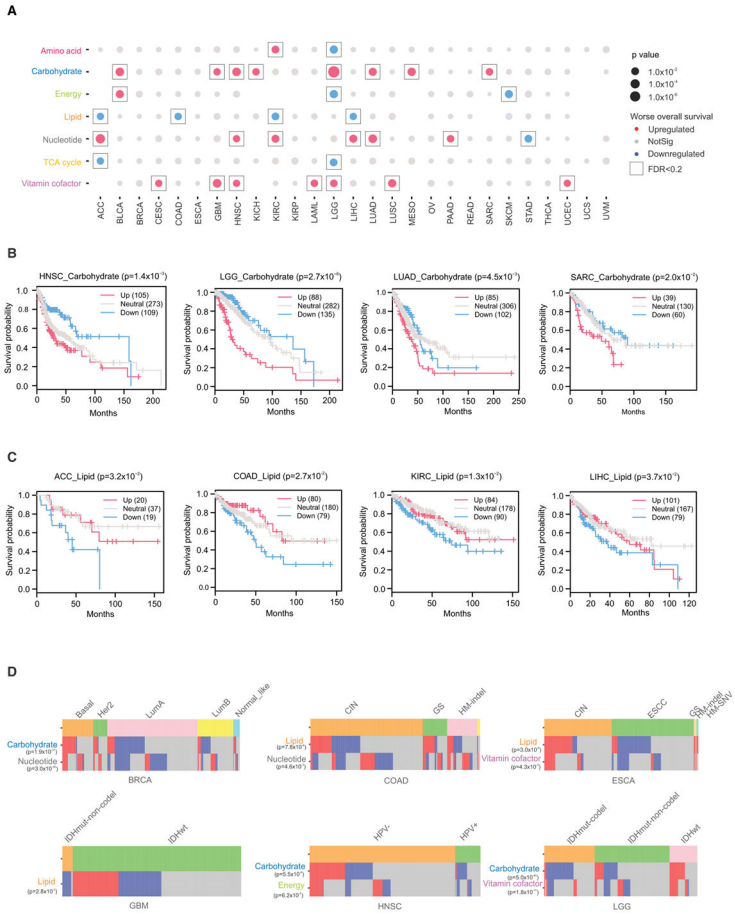

Figure 3. Associations of Metabolic Expression Subtypes with Patient Survival Times and Tumor Subtypes

(A) Clinical associations of metabolic expression subtypes with patient overall survival times. Color indicates the correlation direction; significant correlations (log-rank test, FDR < 0.2) are boxed. Those cases without qualified subtype classifications are left in blank.

(B) Kaplan-Meier plots for carbohydrate metabolic expression subtypes associated with patient overall survival times in head and neck squamous cell carcinoma (HNSC), low-grade glioma (LGG), lung adenocarcinoma (LUAD), and sarcoma (SARC).

(C) Kaplan-Meier plots for lipid metabolic expression subtypes associated with patient overall survival times in adrenocortical carcinoma (ACC), colon adenocarcinoma (COAD), kidney renal clear cell carcinoma (KIRC), and liver hepatocellular carcinoma (LIHC). Cancer type, metabolic expression subtype, and the p value of log-rank test are shown at the top of each plot.

(D) Representative examples of associations between metabolic expression subtypes and established tumor subtypes. p values are based on chi-square test.

See also Figures S2–S4.

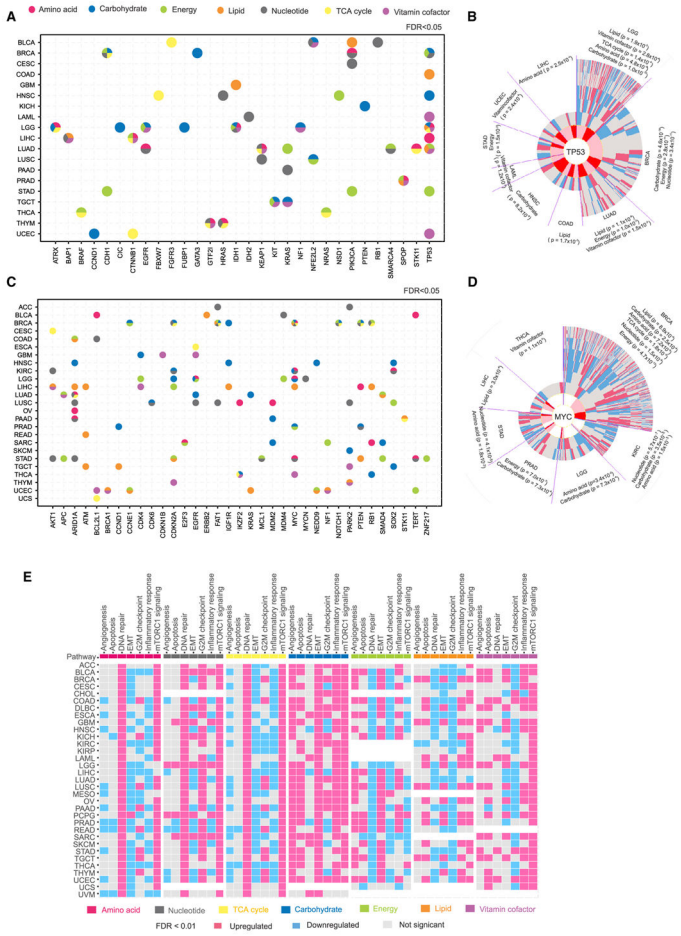

Figure 4. Somatic Drivers and Biological Pathways Associated with Metabolic Expression Subtypes

(A) Somatic mutation drivers associated with metabolic expression subtypes. For each cancer type, the mutational status of significantly mutated genes (identified by MutSigCV, with a mutation frequency > 5%) were assessed based on chi-square test. Colors in each circle indicate the correlations with different kinds of metabolic expression subtypes.

(B) Correlations of metabolic expression subtypes with *TP53* mutation status. The inner band indicates the mutation status of *TP53* (dark red, mutated; light red, wide-type); external bands indicate the subtype information of a specific metabolic pathway (red, upregulated; gray, neutral; and blue, downregulated).

(C) Somatic copy number alteration drivers associated with metabolic expression subtypes. For each cancer type, the copy number status of known oncogenes or tumor suppressors residing in a significant amplification for deletion peak (identified by GISTIC2) were assessed based on chi-square test.

(D) Correlations of metabolic expression subtypes with *MYC* amplification status. The inner band indicates the amplification status of *MYC* (dark red, high-level amplification; light red, low-level amplification); external bands indicate the subtype information of a specific metabolic pathway (red, upregulated; gray, neutral; and blue, downregulated). In (A) and (C), only associations with FDR < 0.05 are shown; color indicates the specific associated metabolic pathway.

(E) Correlations of metabolic expression subtypes with six cancer hallmarks and mTOR signaling pathway based on GSEA (the related gene sets are based on MSigDB). Those cases without qualified subtype classifications are left in blank, and significant enrichments (FDR < 0.01) are colored in red or blue. For the analysis, differentially expressed genes were identified between the upregulated and downregulated subtypes. Red indicates the enrichment of a hallmark gene set in genes highly expressed in the upregulated metabolic expression subtype; blue indicates the opposite pattern.

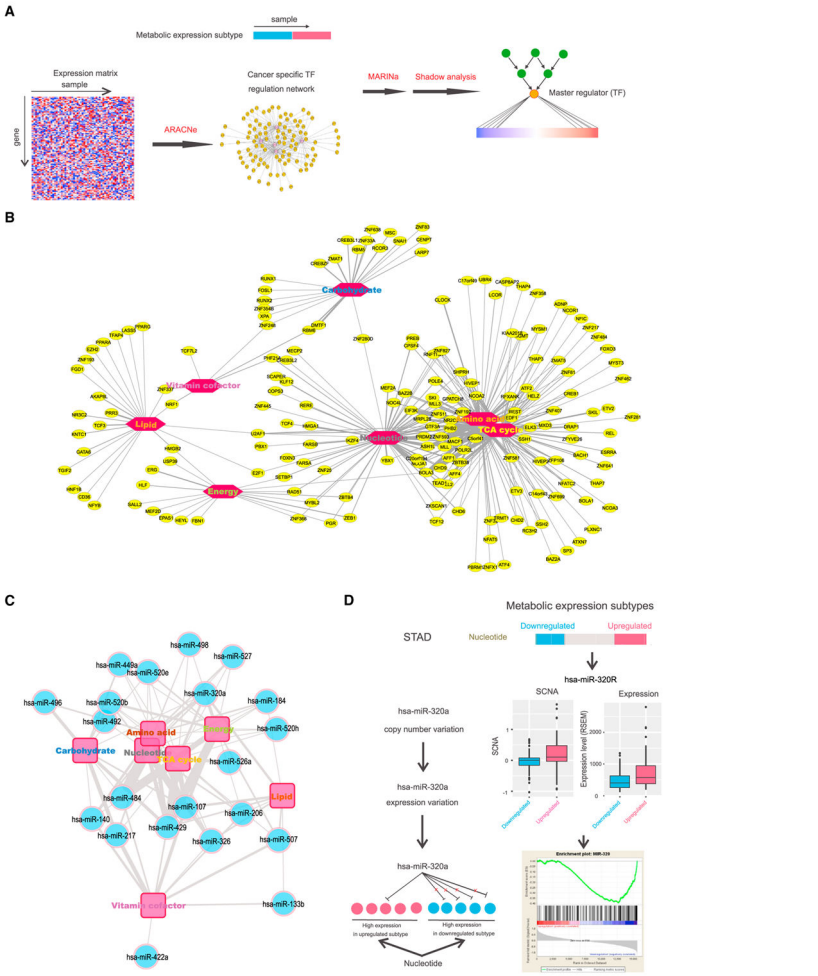

Figure 5. Master Regulators Associated with Metabolic Expression Subtypes

(A) Overview of computational algorithms used to identify master transcription factors.

(B) Network view of “master” transcription factors associated with metabolic expression subtype. The line thickness indicates the number of cancer types where the connection was identified. Only the connections identified in ≥3 cancer types are shown.

(C) Network view of “master” miRNA regulators.

(D) MiRNA hsa-miR-320a identified as a master regulator for expression subtypes of the nucleotide metabolism pathway in stomach adenocarcinoma (STAD). SCNAs of hsa-miR-320a lead to a lower expression in the samples of downregulated subtype. Its target genes are significantly enriched in genes highly expressed in the downregulated subtype. The middle line in the box is the median, and the bottom and top of the box are the first and third quartiles, and the whiskers extend to 1.5× interquartile range of the lower quartile and the upper quartile, respectively.

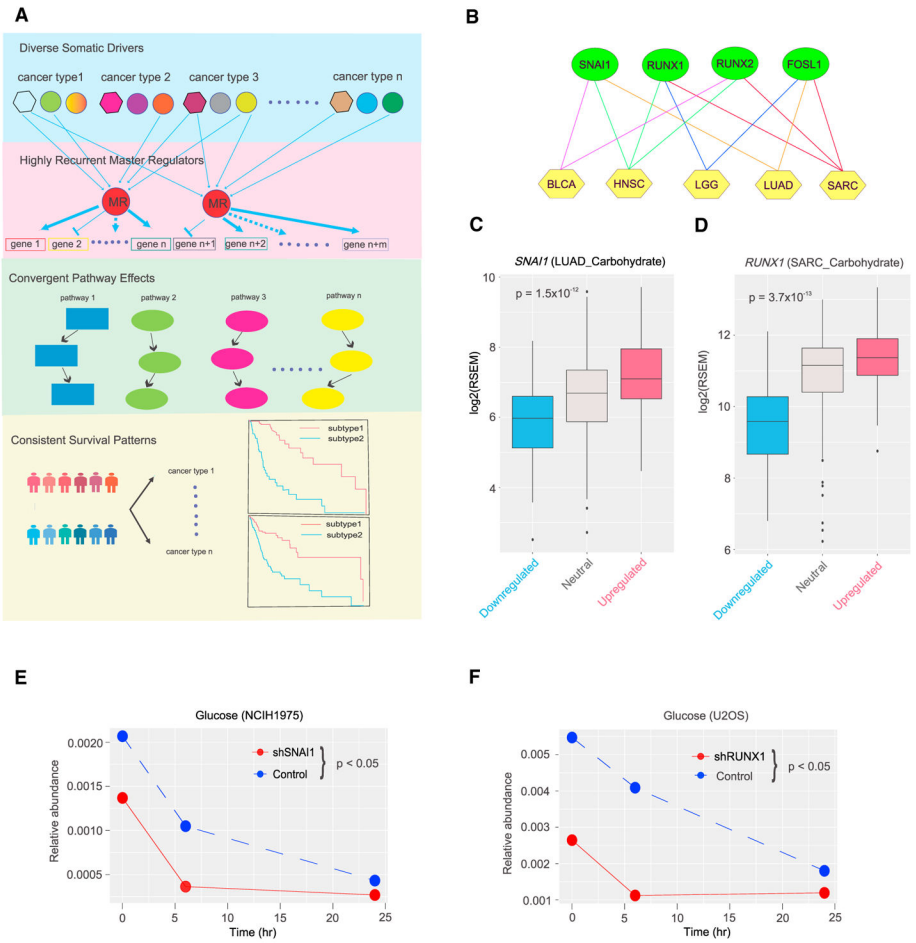

Figure 6. Effects of Master Regulators on Carbohydrate Metabolism

(A) Systematic view of metabolic reprogramming across cancer types.

(B) The network shows that master TFs for carbohydrate metabolism identified in ≥3 cancer types whose upregulated subtypes showed significant worse prognosis, and these master regulators have ≥150 target genes and higher expression levels in the upregulated subtypes.

(C and D) Master regulator expression level in three carbohydrate metabolic expression subtypes: *SNAI1* in lung adenocarcinoma (LUAD) (C) and *RUNX1* in sarcoma (SARC) (D). The middle line in the box is the median, and the bottom and top of the box are the first and third quartiles, and the whiskers extend to 1.5× interquartile range of the lower quartile and the upper quartile, respectively.

(E and F) Relative abundance of intracellular glucose in the NCIH1975 cell line (control) and the cell line with shRNA-mediated *SNAI1* knockdown (E) and in the U2OS cell line (control) and the cell line with shRNA-mediated RUNX1 knockdown (F) at three time points (0 hr, 6 hr, and 24 hr). p value was based on paired t test.

See also Figure S5 and Table S3.

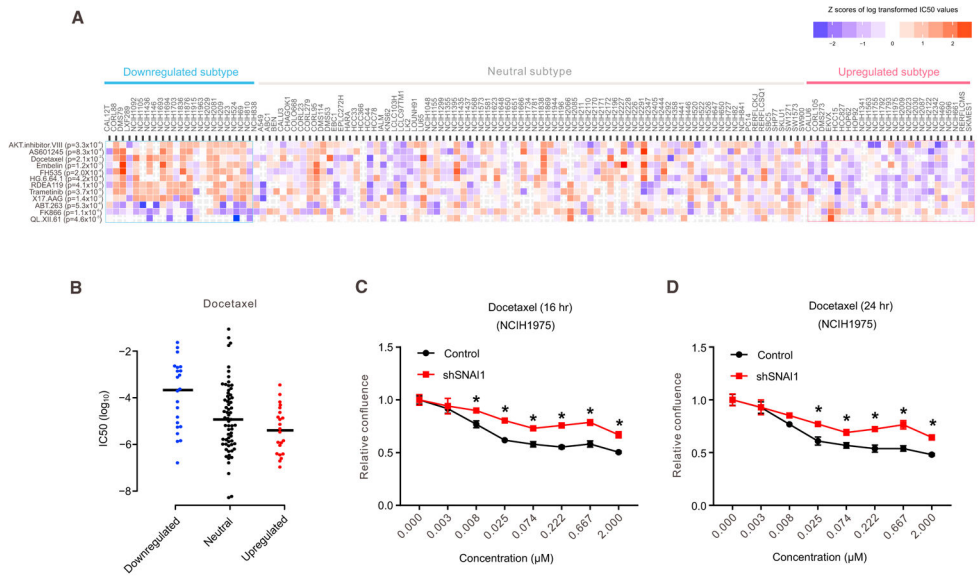

Figure 7. Carbohydrate Expression Subtypes Are Informative about Drug Sensitivity

(A) Heatmap showing drug sensitivity variation across lung cancer cell lines. Those lung cancer cell lines were classified into downregulated, neutral, and upregulated carbohydrate metabolic subtypes using the same method as for TCGA patient samples. All the drugs with a significant difference of IC_{50} (log-transformed) among the three subtypes (FDR < 0.05) are shown.

(B) The distributions showing the log-transformed IC_{50} values of docetaxel in the carbohydrate metabolic expression subtypes.

(C and D) The effect of *SNAI1* knockdown in NCIH1975 cells on drug response of docetaxel at 16 hr (C) and 24 hr (D). Data are represented as mean ± SE. Compared to negative control (scrambled shRNA), *p < 0.05.

See also Figure S6.